International Journal of Engineering and Technology Innovation, vol. 5, no. 4, 2015, pp. 242 – 254

Applications of Differential CDMA Schemes and Control Technology for Distribution Substations

Ching-Chuan Tseng*, Li Wang, and Chih-Hung Kuo

Department of Electrical Engineering, National Cheng Kung University, Tainan, Taiwan, ROC.

Received 03 August 2015; received in revised form 15 September 2015; accepted 20 September 2015

Abstract

This paper presents an approach to achieve monitoring and control of distribution systems in a distribution substation using power-line communication (PLC) combined with Hadamard code. Four different techniques, i.e., binary phase shift keying (BPSK), quadrature phase shift keying (QPSK), 16-quadrature amplitude modulator (QAM) and 64-QAM in code division multiple access (CDMA), are employed. With spreading-spectrum modulation and demodulation in the studied PLC system, the proposed approach can achieve reliable high-speed information transmission through power lines. With Hadamard code, the signals corresponding to different relays are orthogonal to each other and the interference among them can be reduced. The proposed approach has the advantages of high-speed detection, bi-direction communication, reading and backup data, control and turn-off functions, displaying the real-time system information, etc. When 100 kHz is used as the carrier frequency for 256 relays under power-line noise below 14 dB, the simulation results show that the bit error rate (BER) is less than 10^{-5}. The proposed scheme can be applied to the smart-grid distribution substation of the studied distribution systems.

Keywords: power-line communication, binary phase shift keying, quadrature phase shift keying, quadrature amplitude modulator, code division multiple access, bit error rate, orthogonal frequency division multiplexing

1. Introduction

The power-line communication (PLC) has been proposed for information and signal transmission. Owing to the low speed and low quality [1-3] inherited in the PLC systems, its adaptation is limited in the networks from the transformer substations to the customer premises (outdoor) and the private area within the customer buildings (indoor).

Federal Communications Commission (FCC) of USA is currently expanding the feasible frequency range from 2 to 80 MHz, while in Europe, European Telecommunications Standards Institute (ETSI) [4] regulates the frequency ranges from 1.6 to 10MHz for outdoor, and 10 to 30MHz for indoor. These frequency bands are mainly applied to communication network and audio-video (AV) entertainment for the families on PLC. However, Matsumoto [5] made a conclusion that the PLC system with the baud rate of about 5 Mbps was possible for the frequency range from 10 to 450 kHz. In fact, the maximum baud rate of transmitted signal with data can reach 200 Mbps by using techniques to extend the bandwidth.

The PLC systems make use of either code division multiple access (CDMA) or orthogonal frequency division multiplexing (OFDM) to alter the bandwidth efficiency on transmission of data traffic. The comparisons of the communication system using

* Corresponding author. E-mail: tsengx@ee.ncku.edu.tw

OFDM and CDMA [6] were performed under the same conditions including overall baud rate, bandwidth occupation, and equal transmitted power [7]. The narrow-band PLC using low-peak approach fits for the CDMA system in the frequency range from 10 to 450 kHz. The wide-band PLC using chimney approach is suitable for the OFDM system in the frequency range from 2 to 80 MHz.

This paper applies four different techniques, i.e. binary phase shift keying (BPSK), quadrature phase shift keying (QPSK), 16-quadrature amplitude modulator (QAM), and 64-QAM in the CDMA combining Hadamard code with spreading spectrum modulation and demodulation in the PLC systems. The signals corresponding to different relays are orthogonal to each other, and thus the mutual interference among them can be decreased. Therefore, the multi-stream achieves three merits: increase of transmission speed, decrease of transmitted signal power, and extension of bandwidth efficiency. The signals are transmitted at a high speed to achieve long-distance transmission while, in the meantime, both quantities of amplifiers and the value of BER are also reduced. Furthermore, the paper provides a new method enhance security, reliability, and quality to build the distribution substation with high speed for the power distribution system in smart grid.

This paper is organized as follows. Section II introduces the framework of the monitoring and control distribution substations using BPSK, QPSK, 16-QAM, and 64-QAM in CDMA on the PLC systems. Section III describes the system model. Section IV demonstrates the simulation and numerical analysis with discussion. Section V draws the specific conclusions for this paper.

2. Distribution substation using CDMA scheme

2.1. Framework of a Distribution Substation

The circuit framework of a distribution substation of the studied distribution systems may consist of two parts: (a) protecting relay circuits, and (b) monitoring and control circuits. The communication in a traditional distribution substation is accomplished by: (a) power-line carrier, (b) radio carrier, and (c) telephone carrier to achieve safe and reliable distribution automation systems. Fig. 1 shows the block diagram of the framework for monitoring and control of an automatic distribution [8- 9].

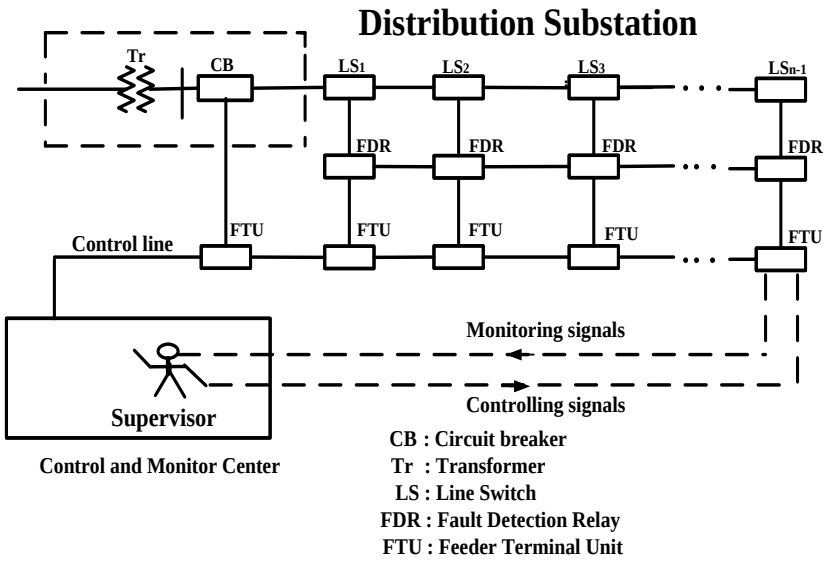

Fig. 1 Traditional 1 × *N* distribution substation

In the conventional operations of a distribution substation, as shown in Fig. 1, the transmitted signals of the switches LS_1, LS_2, …, LS_{n-1} go to the feeder terminal unit (FTU) through the fault detection relay (FDR), while the signal of the circuit breaker (CB) directly goes to FTU. The above signals corresponding to the different relays (including CB relay) for a distribution substation are passed to the monitoring and control center. Moreover, if the supervisor of the monitoring and control center finds abnormal signals at the FDR, the supervisor can send a control signal to the FTU and then to the FDR via a control line in order to turn off the faulted line switch (LS).

This paper proposes a new approach to achieve monitoring and control of the studied distribution substation in order to replace the traditional distribution automation system. This approach accomplishes the goal of monitoring and control of the transmission distribution automation system using four different techniques, i.e. BPSK, QPSK, 16-QAM, and 64-QAM with spreading spectrum modulation and demodulation for the PLC system as shown in Fig. 2.

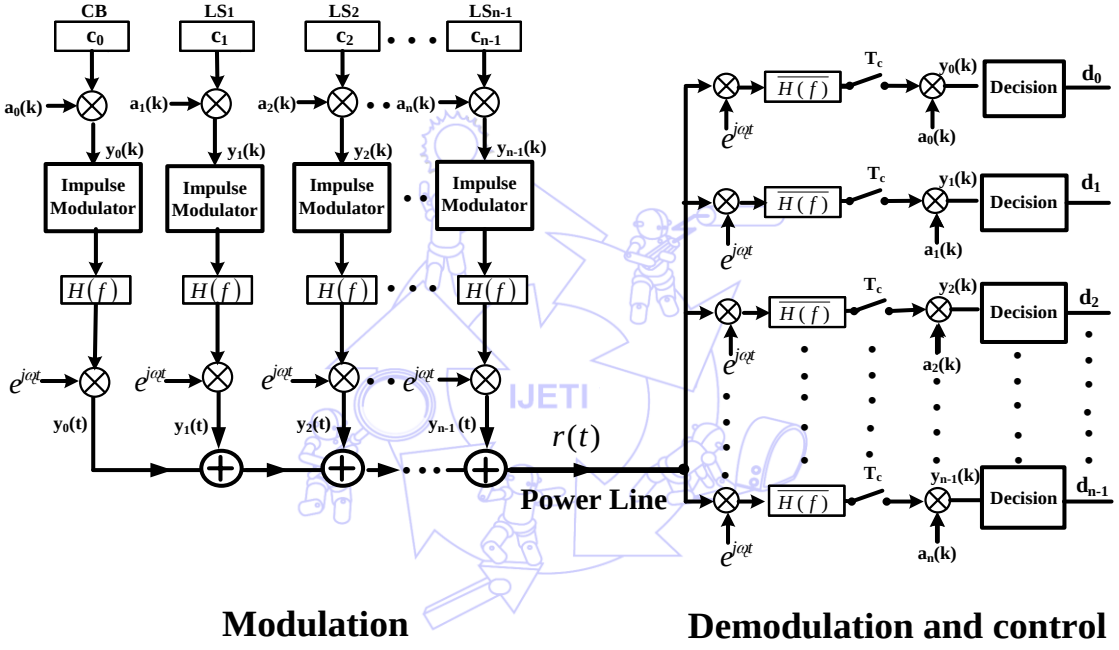

Fig. 2 Schematic configuration 1× *N* of spreading modulation and demodulation

Since Hadamard code has the characteristics that the elements of the core are either +1 or -1, and it can further be expanded to N×N with $N = 2^n$. Taking $n = 2$ as an example, the Hadamard code is shown as below.

$$H_{4\times4} = \begin{bmatrix} 1 & 1 & 1 & 1 \\ 1 & -1 & 1 & -1 \\ 1 & 1 & -1 & -1 \\ 1 & -1 & -1 & 1 \end{bmatrix} \quad (1)$$

Each row in the Hadamard transform corresponds to the different code word from the different relay which represents circuit breaker (CB), Line switch #1 (LS_1), LS_2, …, LS_{n-1} shown in Fig. 1.

2.2 Operation of the Distribution Substation

The signal of the switch (CB) with c_0 is encoded by Hadamard code a0(k) to be y0(k). The signal y0(k) then goes through

Impulse Modulator and the wave shaping filter. After being modulated with carrier frequency, the spreading signal y0(t) is obtained. Following the similar process, y1(t), y2(t), …, yn−1(t) are obtained as shown in Fig. 2. The signal, which is the serial summation of y0(t), y1(t), …, yn−1(t) is transmitted through the transmission power line to the receiving end for demodulation, monitoring, and control in distribution substations. The decision panel compares the reference values (r_0, r_1, …, r_{n-1}), which are referred to the allowed maximum load, i.e., overload, over-voltage, under-frequency, over-frequency, and unbalanced operation such as single phasing, etc. with the transmitted thresholds (c_0, c_1, …, c_{n-1}) for different relays, and the absolute values of δ_0, δ_1, …, δ_{n-1} are obtained, where $\delta_0 = |c_0 - r_0|$, $\delta_1 = |c_1 - r_1|$,…, $\delta_{n-1} = |c_{n-1} - r_{n-1}|$. If δ_0, δ_1, …, or δ_{n-1} is greater than the corresponding maximum allowed initial value, the control signals (d_0, d_1, …, d_{n-1}) will be sent to different relays as well as the supervisor for further performance either monitoring and control of the system or turning off the faulted switch.

2.3 Framework of the PLC Circuit

Since the impedance of the transmission line is uniformly distributed, the inductance and capacitance per unit length of the transmission line depend on the employed conductive materials. The function of the PLC signal with respect to the frequency and the distance can be calculated approximately by

$$H(f) = \sum_{i=1}^{N} g_i \cdot e^{-\alpha(f)\cdot \ell_i} \cdot e^{-j2\pi f \tau_i} \tag{2}$$

where g_i is a weight which depends on the topology of the link, $\alpha(f)$ is the attenuation coefficient that takes into account both skin effect and dielectric loss, τ_i denote the delay associated with the i th path, ℓ_i are the path lengths and N is the number of non-negligible paths.

From equation (2), it is clearly known that the attenuation of the PLC signal is based on frequency and distance with logarithmic distribution. According to the estimation, the PLC signal can be transmitted to a limited distance in a probabilistic sense as shown in Fig. 3 which shows the outdoor coverage predication for four outdoor carrier frequencies (50 kHz, 100 kHz, 150 kHz, and 2.4 MHz) with different probabilities and a standard deviation of 12dB [10].

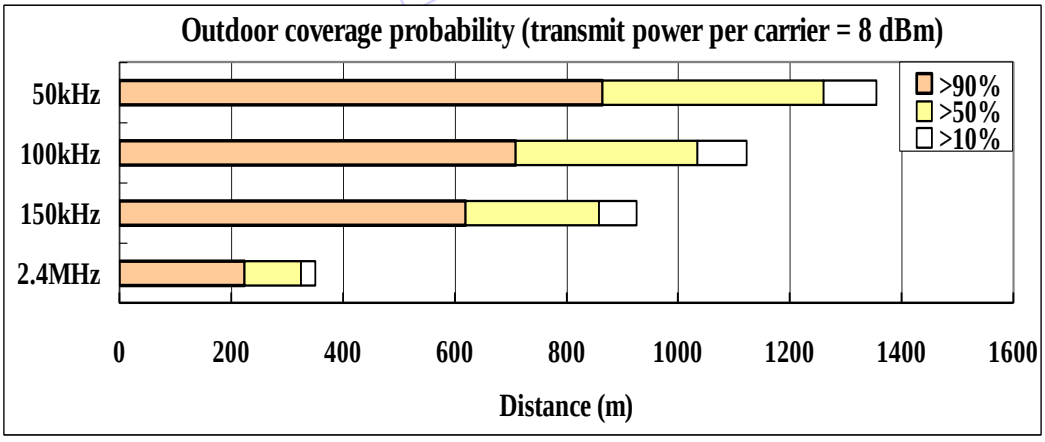

Fig. 3 Outdoor coverage probability with respect to distance for cable link OM-OAP

The coupling unit is composed of a capacitor circuit for coupling communication signals, and an inductor circuit for passing low-frequency high power at signal ports A and B, and a fusible safety link for protecting the coupling capacitor and inductor from the power line as shown in Fig. 4.

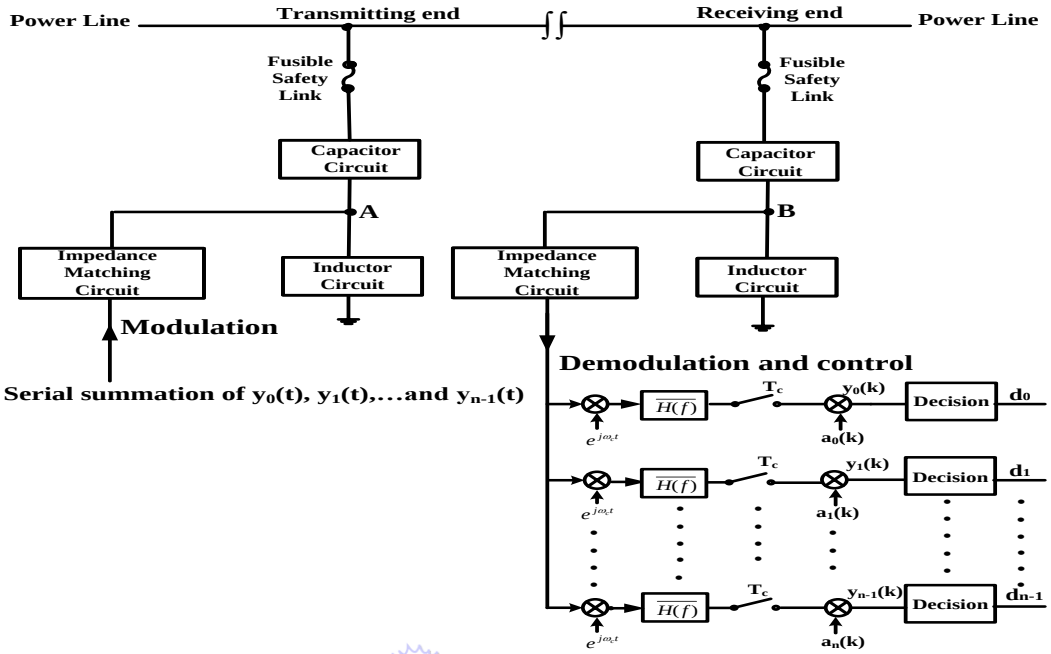

Fig. 4 On-line/download of signals with message on the power line.

The serial summation of $y_0(t)$, $y_1(t)$, …, $y_{n-1}(t)$ at the transmitted end goes through an impedance-matching circuit to point A and then passes through the capacitor circuit to the power line. The above signals at the receiving end pass through the capacitor circuit to point B and then pass directly through the impedance-matching circuit to its own receiver port for checking control and turning off the faulted switch shown in Fig. 4.

The signals attenuate with the increase of the transmitted distance in logarithmic form and, hence, they have to be amplified as shown in Fig. 5. The inductor circuit between points A and B is for low-frequency signals, and the bi-directional amplifier circuit can be used in bi-directional link port transmission between points C and D. The signals appearing at point A go through the capacitor circuit between points A and C to the bi-directional amplifier circuit [11]. The amplified signals are divided into two paths: (a) the normal path on which the signals appearing at point D pass through the capacitor circuit to point B, and (b) the abnormal path on which the amplified control signals (d_0, d_1, …, d_{n-1}) appearing at point C pass through the capacitor circuit to point A, and then go through the power line to be transmitted.

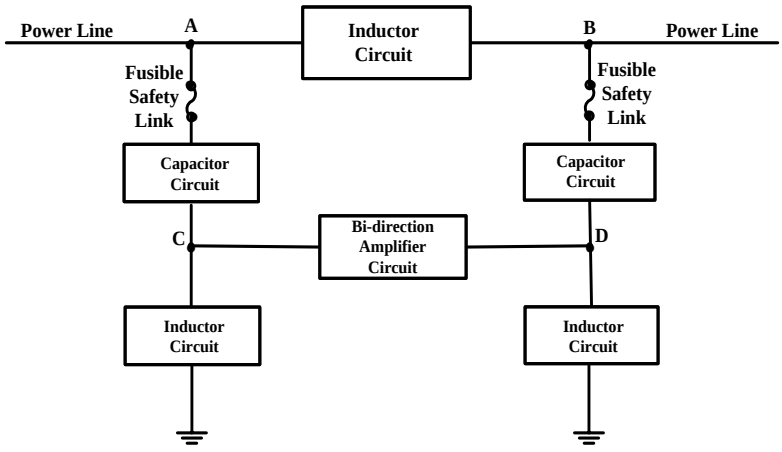

Fig. 5 Signals with data amplified on the power line.

The signal attenuation depends on the power losses of the path and the variations of the power-line noise. The power losses of the path are dependent on the cable type, cable length, coupling mismatch number, and the number of branches on the power-line network. The path losses increase with the increase of frequency and distance, while the power-line noise decreases with the increase of frequency. Fig. 3 showed the probability density function of the signal with respect to the distance in logarithm form. The three probability distributions (90 percent, 50 percent, and 10 percent) are expressed by three different grey levels, respectively, with respect to the distance on the power line. For example, the 100 kHz with probability of 90 percent within 710 m is to be amplified.

3. System Model

A new approach is proposed in this paper for the PLC system using CDMA as the system model with the same parameters for all analyses and simulations in order to achieve monitoring and control of the distribution substations. The transmitted signals pass through multiple paths with mutual interference, narrowband interference, and additive white Gaussian noise (AWGN) through an asynchronous CDMA system [12-13]. The signal at channel modulation output is given by

$$r(t) = \sum_{i=0}^{m-1} y_i(t) + n(t) \tag{3}$$

where i denotes the index of the users corresponding to different switches (CB, LS_1, LS_2, …, LS_{n-1}) for the studied distribution substation and n(t) is the PLC noise which is mainly the AWGN that is mostly composed of the zero mean complex Gaussian noise, and $y_i(t)$ sequence is the spreading signals of m users with a narrow bandwidth R_s which is to be spread to a wide bandwidth R_c. The spreading factor SF is defined as $SF = N = R_c/R_s = T_s/T_c$, where R_c, R_s, T_s, and T_c are the chip rate, the symbol rate, the chip period, and the symbol period, respectively.

The variance of the AWGN waveform $n(t)$ depends on both time and frequency and the $n(t)$ can be represented by

$$\sigma^2(t, f) = \sigma^2(t)a(f) \tag{4}$$

where

$$\sigma^2(t) = \sum_{j=1}^{3} A_j \left|\sin(2\pi f_c t + \varphi_j)\right|^n \tag{5}$$

and

$$a(f) = \frac{e^{-af}}{\int_0^{f_s} e^{-af} df} \tag{6}$$

The function $\sigma^2(t)$ in equation (5) indicates the instantaneous power of the noise, and $a(f)$ in equation (6) denotes the power spectral density normalized by the total noise power in the frequency ranges from 0 to f_s, where f_s is occupied bandwidth.

Table 1 lists the parameters collected within one period (T_{ac}) of the alternating current [14, 15]. If the transmitted signal is assumed without loss of generality, we can assume that an asynchronous CDMA system with spreading factor N allows the users

to have random access on the uplink fading channel by combining AWGN. The received signal through a band-pass filter of the receivers at the carrier frequency f_c is given by

$$r(t) = s(t) + n(t) \tag{7}$$

in which $n(t)$ is a zero mean complex Gaussian noise and

$$s(t) = \sum_{k=1}^{K}\sum_{m=1}^{N}\sqrt{2P_s}\, b_{k,m} g(t - kT_s) e^{j(2\pi ft+\varphi)} \tag{8}$$

where the constant P_s is the signal power, the integer $k=T_{ac}/(2T_s)$, and $b_{k,m}$ is the k-th symbol of the user m in the spreading sequence. Using different modulation schemes, the symbols correspond to different $b_{k,m}$, i.e. $b_{k,m} \in \{\pm 1\}$ for BPSK and $b_{k,m} \in \{\pm 1, \pm j\}$ for QPSK. Moreover g(t) is a rectangular pulse

$$g(t) = \begin{cases} 1, & 0 \le t \le T_s \\ 0, & \text{otherwise} \end{cases} \tag{9}$$

For M-Ary modulation schemes like M-PSK including BPSK, the energy in a symbol is the sum of the signal power of the in-phase and quadrature phase components. Relationship between the signal power (P_s) and the symbol energy (E_s) is given by

$$E_s = R_m R_c P_s \tag{10}$$

where E_s and R_c are the symbol energy per modulated bit and chip rate, respectively, while $R_m = \log_2(M)$, where $M = 2$ for BPSK, $M = 4$ for QPSK, $M = 16$ for 16-QAM, etc.

Table 1 Noise parameters

j	A_j	φ_j[deg.]	n_j	a
1	0.13	–	0	8.8×10^{-6}
2	0.26	128	9.3	
3	16	161	6.9×10^{3}	

The received signals pass through matched filters to their own receiver ports at the carrier frequency of f_c, as shown in Fig. 2. The sample in the k-th symbol at $t = kT_s$ for the m-th user is represented by

$$r_{k,m} = \left[r(t) e^{j(2\pi ft+\phi)} * g(t) \right]_{t=\kappa T_s} = s_{k,m} + n_{k,m}. \tag{11}$$

where the symbol $*$ denotes the convolution operation and the components of the signal and the noise are expressed as $s_{k,m}$ and $n_{k,m}$, respectively.

The signal $s_{k,m}$ in equation (11) is the spreading sequence of user m at the k-th symbol in a short duration of $kT_s \le t \le (k+1)T_s$, and it can be expressed as

$$s_{k,m} = \int_{-\infty}^{\infty} s(t) g(t - kT_s) e^{-j(2\pi ft+\varphi)} dt = \int_{kT_s}^{(k+1)T_s} s(t) e^{-j(2\pi ft+\varphi)} dt = \sqrt{2P_s} T_s b_{k,m} \tag{12}$$

Similarly, the complex Gaussian noise signal $n_{k,m}$ with zero mean is represented as

$$n_{k,m} = \int_{-\infty}^{\infty} n(t)g(t-kT_s)e^{-j(2\pi ft+\varphi)}dt \tag{13}$$

A suitable linear model with zero mean complex Gaussian and variance $\sigma_{k,m}$ is selected as the channel noise. The variance $\sigma_{k,m}$ is expressed as

$$\sigma_{k,m}^2(t) = E\left[n_{k,m}^2\right] = \alpha(f)\int_{kT_s}^{(k+1)T_s}\sigma^2(t)dt \tag{14}$$

The average noise power in a short duration of $-T_{ac}/2 \le t \le T_{ac}/2$ is given by

$$P_n = \int_{-T_{ac}/2}^{T_{ac}/2}\sigma^2(t)dt = \frac{2}{T_{ac}}\int_0^{T_{ac}/2}\sigma^2(t)dt \tag{15}$$

The BER for $r_{k,m}$ can be evaluated by

$$P_{k,m} = \frac{1}{\sqrt{2\pi}\sigma_{k,m}}\int_0^{\infty} e^{-\frac{(x+\sqrt{2P_s}T_{sc})^2}{2\sigma_{k,m}^2}}dx = \frac{1}{2}erf\left(\sqrt{\frac{P_sT_{sc}^2}{4\sigma_{k,m}}}\right) \tag{16}$$

From the above equations (10) and (16), the probability of bit error in M-QAM is derived [16] by the following modified formula:

$$P_b(M) = \frac{\sqrt{M}-1}{2\sqrt{M}\cdot\log_2\sqrt{M}}erfc\left(\sqrt{\frac{3\log_2 M\cdot P_s\cdot T_{sc}^2}{8(M-1)\cdot\sigma_{k,m}}}\right) \tag{17}$$

where $erfc$ (x) is the complementary error function.

4. Results and Discussions

The PLC system using four different modulation schemes, i.e. BPSK, QPSK, 16-QAM, and 64-QAM, under P/P_n=7 dB has different BER values that are calculated by using equation (16) with parameters obtained from the noise parameters listed in Table 1 and the system parameters listed in Table 2. Using the carrier frequency of 100 kHz, the Fig. 6 shows BER performance as function of time, and hence the number of symbols per $T_{ac}/2$ is 250 in interval of the time from 0 to $T_{ac}/2$. This numerical methodology with equation (16) and Katayama [7] will be applied to the PLC system using the above mentioned system parameters with different techniques, i.e. OFDM, CDMA for the analysis and comparison. As above numerical result, while the BER value less 10^{-5}, the optimal carrier frequency range is chosen to be 204- kHz, 90- kHz, 110- kHz, 150- kHz, and 270- kHz on the PLC system using five OFDM, BPSK, QPSK, 16-QAM, and 64-QAM, respectively.

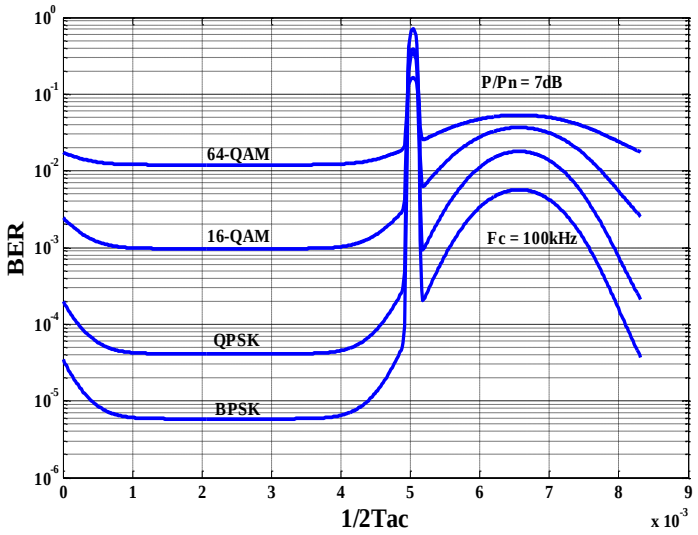

Fig. 6 BER values using BPSK, QQPSK, 16-QAM, and 64-QAM under carrier frequency of 100 kHz and P/P_n=7.

Table 2 System parameters

Modulation schemes	BPSK, QPSK, 16-QAM and64-QAM
Alternating-current period (T_{ac})	1/60 = 16.666 ms
Carrier frequencies (f_c)	10-300 kHz
Spreading factor	16-256
Symbols	250
Chip rate	2×10^4
T_c	5×10^{-5}
T_s	1.28×10^{-2}
Samples per chip	50

For the PLC system with 256 users, the chip spectrogram of the signal with the AWGN under input signal to noise ratio (SNR) of -14 dB is transmitted in the channel. The power of the noise decreases with the increase of the carrier frequency as shown in Fig. 7. Similarly, relationship between the BER and the carrier frequencies for PLC system using the BPSK-CDMA system with five different users under the power-line noise below 14 dB is shown in Fig. 8 (a). As mentioned above, they fit the results mentioned in Section 2.3. Simultaneously, relationship between the BER and the carrier frequencies for PLC system with 256 users using four different BPSK, QPSK, 16-QAM, and 64-QAM under the carrier frequencies ranging from 10 kHz to 90 kHz is shown in Fig. 8 (b).

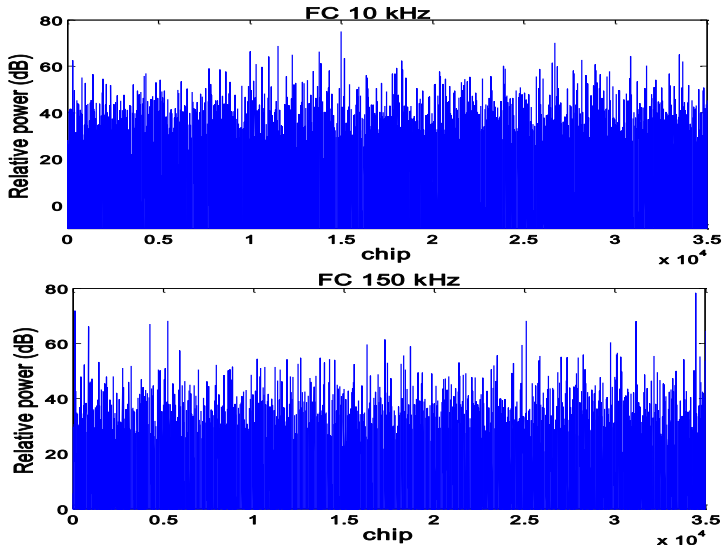

Fig. 7 Signal in AWGN channel with respect to frequencies 10 kHz and 150 kHz.

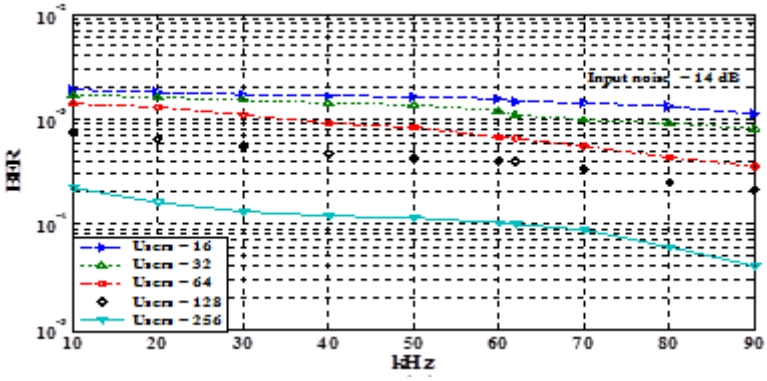

(a) the system with variable users using BPSK

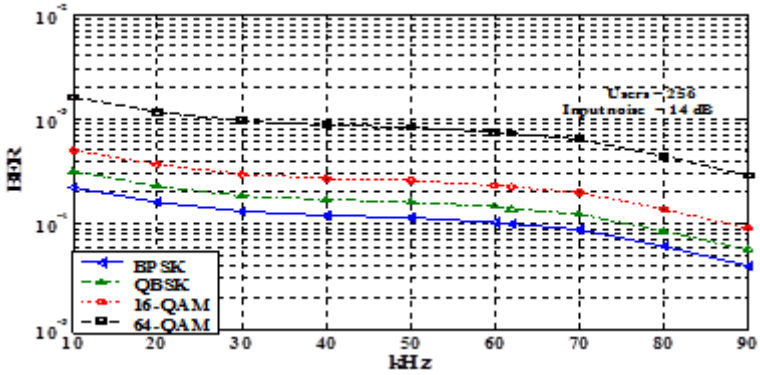

(b) the system with 256 users using BPSK, QPSK, 16-QAM, and 64-QAM

Fig. 8 Relationship between the BER and the carrier frequencies for PLC system

The mean BER values averaged by repeating simulation more than 100 times for the PLC system with 256 users using BPSK, QPSK, and 16-QAM under the same system parameters with carrier frequency ranging from 10 kHz to 200 kHz, and the same power-line noise below 14 dB are shown in Fig. 9. In a certain carrier frequency range, the BER value using equation (16) of BPSK can fit closely with the BER value obtained by simulations using BPSK. As a result, with SNR ranging from -16.32 dB to -10 dB for the PLC system, the BER values corresponding to BPSK, QPSK, 16-QAM, and 64-QAM using two carrier frequencies of 100 kHz and 150 kHz decrease from 10^{-3} to 10^{-9}, as shown in Fig. 10 [17].

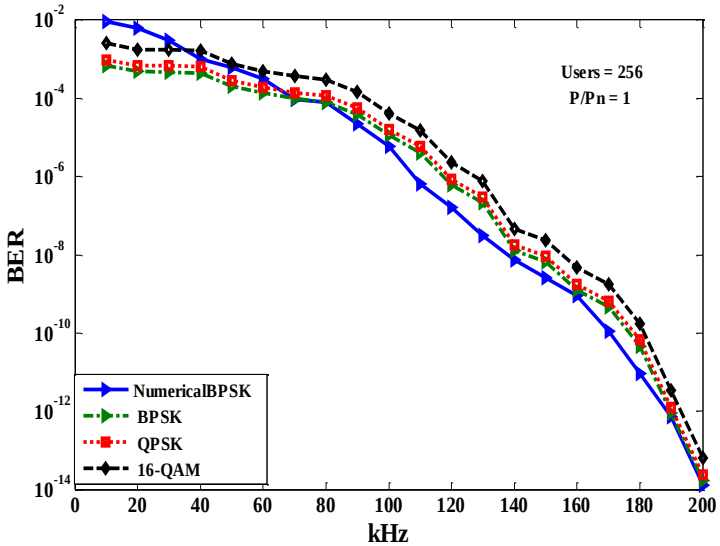

Fig. 9 BER values corresponding to different carrier frequencies using Numerical BPSK, BPSK, QPSK, and 16-QAM

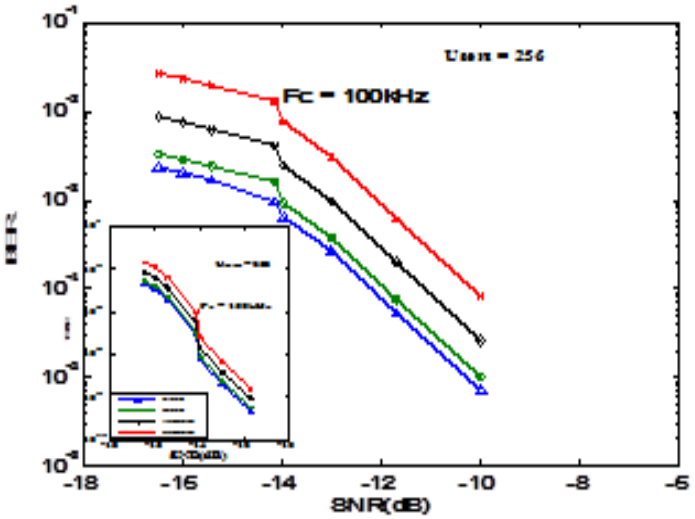

Fig. 10 BER values using BPSK, QPSK, 16-QAM, and 64-QAM as a function of short-term average SNR under carrier frequency of 100 kHz and 150 kHz

In the above results, the choice of an optimal carrier frequency for the studied PLC system is determined by less BER value and long transmitted distance as expected. Fig.3, Fig.9, and Fig.10 show the relationship among the transmitted distance, optimal carrier frequency, and power-line noise of the studied PLC system, respectively. As the carrier frequency increases, the PLC system combining Hadamard code will achieve less BER value, and the effect of the power-line noise will be less. On the contrary, the transmitted distance is decreased in logarithmic form and the amplifier quantities are increasing in the PLC system when the carrier frequency increases. As mentioned above, Table 3 is selected optimal carrier frequency range and transmitted distance to achieve the relative comparisons among BPSK, QPSK, 16-QAM, and 64-QAM for the PLC systems.

Table 3 Relative comparisons among BPSK, QPSK, 16-QAM, and 64-QAM

Item	BPSK	QPSK	16-QAM	64-QAM
Approach 10-5 of BER values	70-130 kHz	80-130 kHz	90-130 kHz	100-140 kHz
Transmitted distance	778 to 641 m	748 to 641 m	722 to 641 m	699 to 625 m
Bandwidth	60 kHz	50 kHz	40 kHz	40 kHz

In this example, when the PLC system with 256 users uses BPSK, QPSK, and 16-QAM under the carrier frequency of 100 kHz and power-line noise below 14 dB, the transmitted distance is approximate 699 m as BER values are less than 10^{-5}. In this way, the PLC system will be utilized frequently and it may also be employed in high-voltage distribution substation or transmission line in harsh environment, e.g. the operation of nuclear reactor or chemical reactor. Furthermore, the proposed PLC system may be applied to multimedia and digital communication, compressed data transmission, and smart grid of distribution substation for different electric power systems.

5. Conclusions

This paper has proposed a PLC system combined with Hadamard codes to obtain high-speed transmission capability. The proposed PLC system employs modulation/demodulation schemes of BPSK, QPSK, 16-QAM, and 64-QAM in CDMA by transmitting up- and down-link information to achieve monitoring and control of a distribution substation in a power distribution system. The performance of the proposed PLC system is evaluated under different values of carrier frequency, number of users, power-line noise and different scheme. The proposed PLC system with advanced supervisory control and data acquisition (SCADA) ability can be used to replace conventional PLC system. Using experiment noise spectrum in Table 1 and

system parameters in Table 2, the PLC system combining Hadamard code with different scheme is obtained. As the experiment results are compared with the ones proposed by Katayama [7] to show Table 4.

Table 4 Characteristic comparisons among experiment results and Katayama [7]

Item	OFMA	BPSK	QPSK	16-QAM	64-QAM
Approach 10-5 of BER values	204- kHz	70-130 kHz	80-130 kHz	90-130 kHz	100-140 kHz
Transmitted distance	≦517 m	≦778 m	≦748 m	≦722 m	≦699 m
Suitable bandwidth	wide-band	narrow-band	narrow-band	narrow-band	narrow-band
BER values	$\leqq 10^{-5}$	$\leqq 10^{-5}$	$\leqq 10^{-5}$	$\leqq 10^{-5}$	$\leqq 10^{-5}$

Implementation of power line technology provides many advantages connective either optical fiber or wireless, e.g., low installation cost, less BER($\leqq 10^{-5}$), transmitted distance(≧778 m), reduced interference among them, lower signal power, etc. However, the distribution substation using hybrid mixing PLC/ optical fiber combining wireless communication schemes has certain challenges and opportunities, which need to be addressed for its future use in Smart Grid environment.

References

[1] G. Jee, C. Edison, R. D. Rao and Cern, "Demonstration of the Technical Viability of PLC Systems on Medium and Low-Voltage Lines in the United States," IEEE Communications Magazine, pp. 108-112, May 2003.

[2] M. Götz., M. Rapp and Dostert, "Power Line Channel Characteristics and Their Effect on Communication System Design," IEEE Communications Magazine, vol. 42, no. 2, pp. 78-86, April 2004.

[3] K. Destert, "Telecommunications over the Power Distribution Grid-Possibilities and Limitations," Proc. 1st International Symposium on Power Lines Communications and it Application (ISPLCA 1997), Apr. 1997, pp. 1-9.

[4] ETSI TS 101 867 v1.1.1, "Powerline Telecommunications (PLT); Coexistence of Access and In-House Powerline Systems," European Telecommunications Standards Institute, pp. 1-11, 2000.

[5] W. Matsumoto, "The Power Line Communication Modem by the Dispersed Tone Modulation Method which is Applied Multicarrier Data Transmission Technology," IEICE Trans, vol. J84-B, no. 1, pp. 38-49, 2001.

[6] Re, E. Del., R. Fantacci, S. Morosi, and Seavalle, "Comparison CDMA and OFDM Techniques for Downstream Power-Line Communications on Low voltage Grid," IEEE Trans. on Power Delivery, vol. 18, no. 4, pp. 1104-1109, 2003.

[7] M. Katayama, "Introduction to Robust, Reliable, and High-Speed Power-Line Communication System," IEICE Trans., vol. E84-A, no. 12, pp. 2958-2965, 2001.

[8] C. C. Tseng, J. F. Chen, and C. H. Kuo, "Monitoring and Controlling Power Generators in Underwater Environment Using CDMA on Acoustic Communication and Power Line Communication", Proc. Symposium on Ultrasonic Electronics, vol. 35, Dec. 2014, pp. 351-352.

[9] C. S. Chen, C. H. Lin, H. J. Chuang, C. S. Li, M. Y. Huangm and C. W. Huang, "Optimal Placement of Line Switches for Distribution Automation Systems Using Immune Algorithm," IEEE Trans. on Power Systems, vol. 21, no. 3, pp. 1209-1217, 2006.

[10] W. Liu, H. Widmer, Raffin, "Broadband PLC Access Systems and Field Deployment in European Power Line Networks," IEEE Communication Magazine, pp. 114-118, May 2003.

[11] M. H. Oxrnan, "Bi-directional Signal Circuit," Patent US3175050, 1965.

[12] M. Toriak and G. Xu, "Blind Multiuser Channel Estimation in Asynchronous CDMA Systems," IEEE Trans. on Signal Processing, vol. 45, pp. 137-147, 1997.

[13] P. B. Rapajic and B. S. Vucetic, "Adaptive Receiver Structures for Asynchronous CDMA Systems," IEEE Journal on Selected Areas in Communications, vol. 12, no. 4, pp. 685-692, 1994.

[14] M. Katayama, S. Itou, T. Yamazatot and A. Ogawa, "Modeling of Cyclostationary and Frequency Dependent Power Line Channels for Communications," Proc. International Symposium on Power Line Communication and its Application (ISPLCA 2000), Apr. 2000, pp. 123-130.

[15] M. Katayama, T. Yamazato and H. Okada, "A Mathematical Model of Noise in Narrowband Power Line Communication Systems," IEEE Journal on Selected Areas in Communications, vol. 24, no. 7, pp. 1267-1276, 2006.

[16] J. C. Cartledge and J. D. Downie, "Long-Haul Performance of 112 Gb/s PM-QPSK: Implications of Enhanced Optical Fiber Transmission Properties," IEEE Journal of Light wave Technology, vol. 30, no. 24, pp. 3771-3779, 2012.

[17] T. Ebihara, "Improvement of Power Efficiency for Underwater Acoustic Communication Using Orthogonal Signal Division Multiplexing over Multiple Transducers," Japanese Journal of Applied Physics, vol. 52, pp. 07GG04-1-07GG04-8, 2013.